Bol. Soc. Paran. Mat.
©SPM – E-ISSN-2175-1188
SPM: www.spm.uem.br/bspm

(3s.) **v. 2026 (44) 10** : 1–19.
ISSN-0037-8712
doi:10.5269/bspm.78851

A Robust Direct Block Hybrid Method for Solving Nonlinear Second-Order Differential Equations

Zakaria Idriss Ali, Freeman Nyathi and Thaithai Sekgobela

ABSTRACT: This paper introduces a robust Block Hybrid Method (BHM) for the direct numerical integration of second-order nonlinear ordinary differential equations (ODEs), with a particular focus on the generalized Van der Pol and Duffing equations. By avoiding the common practice of reducing the problem to a larger first-order system, our method minimizes computational overhead and potential error accumulation. The one-step, self-starting nature of the block formulation provides solutions at multiple grid points simultaneously, enhancing computational efficiency over traditional step-by-step methods. We first establish a priori bounds for the solutions under general conditions to ensure theoretical soundness. The method's efficacy is then validated against several well-known nonlinear problems, demonstrating its high order of accuracy and stability. The results establish the BHM as a highly competitive and reliable alternative for obtaining accurate solutions to second-order initial value problems in applied science and engineering.

Keywords: Block hybrid method, generalized Van der Pol Equation, Duffing equation, Second-Order ODEs, direct method, numerical solution, a priori estimates, stability analysis.

Contents

1. Introduction

Differential equations (DEs) are fundamental to modeling dynamic phenomena across various fields, including engineering, physics, and biology. While linear DEs are often solvable analytically, many real-world systems exhibit complex, nonlinear behavior that necessitates the use of numerical methods. Among the most studied nonlinear DEs are the Van der Pol and Duffing equations, which model systems with nonlinear damping and restoring forces, respectively. These equations are canonical examples of self-sustaining oscillations and chaotic dynamics [9] and [10].

A standard approach for solving second-order initial value problems (IVPs) is to first reduce them to a system of first-order DEs. While effective, this technique increases the dimensionality of the problem, leading to greater computational cost and potential accumulation of numerical errors. To overcome these limitations, direct numerical methods that solve second-order IVPs without reduction have gained significant attention.

The Block Hybrid Method (BHM) has emerged as a particularly powerful direct method [3] and [12]. Unlike traditional linear multistep methods, BHMs are one-step and self-starting, calculating the solution at several points within a block simultaneously. This parallel computation enhances efficiency and allows for straightforward implementation of adaptive step-size strategies. The literature contains numerous

2020 *Mathematics Subject Classification:* 34C15, 70-08, 65L06, 65L05, 34A34.
Submitted September 08, 2025. Published April 17, 2026

Typeset by $\mathcal{B}^{S}\mathcal{P}_{\mathcal{M}}$ style.
© Soc. Paran. de Mat.

developments and applications of BHMs for various orders of IVPs [4], [14], [15] and [18], demonstrating their robustness and accuracy.

In this work, we develop and apply a direct BHM for a generalized form of second-order nonlinear ODEs, encompassing the Van der Pol and Duffing oscillator models. Our primary contributions are threefold:

1. We establish the theoretical foundation for the generalized problem by proving a priori bounds on the solution and its derivative under a set of relaxed conditions.

2. We derive a direct BHM for second-order ODEs and integrate it with a Quasi-Linearization Method (QLM) to effectively handle the nonlinear terms.

3. We demonstrate the method's superior accuracy, efficiency, and stability through extensive numerical experiments on challenging nonlinear problems, comparing our results with exact solutions and established methods from the literature.

This paper is organized as follows: Section 2 formulates the generalized problem and states the necessary assumptions. Section 3 provides the theoretical analysis, establishing a priori estimates for the solution. Section 4 details the derivation of the direct BHM for second-order IVPs. Section 5 presents numerical experiments to validate the method, and Section 6 concludes with a summary of our findings.

2. Problem Formulation and Assumptions

We consider the generalized second-order nonlinear Van der Pol type equation of the form:

$$f_1(t)y''(t) + f_2(t,y)y'(t) + f_3(t,y)y(t) + f_4(t,y) = f_5(t,y), \quad t \in [t_0, T] \tag{2.1}$$

subject to the initial conditions $y(t_0) = y_0$ and $y'(t_0) = y_1$.

This general form encapsulates a wide range of important physical models, see the manuscript [6] for additional information. For instance, by setting $f_1(t) = 1$, $f_2(t,y) = \varepsilon(y^2 - 1)$, $f_3(t,y) = 1$, and $f_4(t,y) = 0$, we recover the classic forced Van der Pol oscillator. Similarly, the Duffing equation is obtained with appropriate choices for the functions f_i.

For our theoretical analysis to hold, we impose the following conditions on the coefficient functions.

Assumption 2.1 (Properties of f_1) *The function $f_1(t)$ is continuous, differentiable, and strictly positive. That is, there exist constants $c_1, C_1, C_{1d} > 0$ such that for all $t \in [t_0, T]$:*

$$0 < c_1 \le f_1(t) \le C_1 \quad \textit{and} \quad |f_1'(t)| \le C_{1d}.$$

Assumption 2.2 (Properties of f_2) *The function $f_2(t,y)$ represents a damping term and is bounded below by a positive constant $c_2 > 0$:*

$$f_2(t,y) \ge c_2 > 0 \quad \forall t \in [t_0, T], \forall y \in \mathbb{R}.$$

Assumption 2.3 (Coercivity of the Restoring Term) *The function $f_3(t,y)$ acts as a restoring force and is uniformly positive. That is, there exists a constant $c_3 > 0$ such that:*

$$f_3(t,y) \ge c_3 > 0 \quad \forall t \in [t_0, T], \forall y \in \mathbb{R}.$$

Assumption 2.4 (Growth Conditions on f_3, f_4, f_5) *The functions f_3, f_4, and f_5 are continuous and satisfy a linear growth condition. That is, there exist positive constants C_3, C_4, C_5 such that for all $t \in [t_0, T]$ and $y \in \mathbb{R}$:*

$$|f_3(t,y)| \le C_3(1 + |y|),$$
$$|f_4(t,y)| \le C_4(1 + |y|),$$
$$|f_5(t,y)| \le C_5(1 + |y|).$$

These assumptions are general enough to cover a wide class of physical oscillators while ensuring that the system is well-behaved, possessing dissipative and restorative properties that prevent solutions from growing unbounded. Having introduced the necessary assumptions, we can now derive the estimates required on the solution and its derivative.

3. A Priori Estimates for the Solution

In this section, we establish a priori bounds for the solution of the generalized problem (2.1). This theoretical result guarantees that the solution and its derivative remain bounded over the time interval, which is a prerequisite for the stability of any numerical scheme.

Theorem 3.1 *Let $y(t)$ be a solution to Equation (2.1) on the interval $[t_0, T]$. Under Assumptions 2.1-2.4, there exists a constant $C > 0$, which depends on the initial conditions, T, and the constants from the assumptions, such that the following a priori estimate holds:*

$$\sup_{t\in[t_0,T]} |y(t)|^2 + \sup_{t\in[t_0,T]} |y'(t)|^2 \leq C.$$

Proof: The proof proceeds in two main steps. First, we establish a bound on $y'(t)$ using an energy method, which will depend on an integral involving $y(t)$. Second, we establish a bound on $y(t)$ itself, thereby closing the estimate. We first deal with the estimate for y'.

Bounding the derivative $y'(t)$.

We multiply Equation (2.1) by $y'(t)$ and integrate from t_0 to an arbitrary $t \in [t_0, T]$:

$$\int_{t_0}^{t} f_1 y'' y' ds + \int_{t_0}^{t} f_2 (y')^2 ds + \int_{t_0}^{t} f_3 y y' ds = \int_{t_0}^{t} (f_5 - f_4) y' ds. \tag{3.1}$$

We estimate each term. For the first term, we use integration by parts:

$$\int_{t_0}^{t} f_1 y'' y' ds = \int_{t_0}^{t} f_1 \frac{1}{2} \frac{d}{ds} (y')^2 ds = \frac{1}{2} f_1(t) |y'(t)|^2 - \frac{1}{2} f_1(t_0) |y'(t_0)|^2 - \frac{1}{2} \int_{t_0}^{t} f_1'(s) |y'(s)|^2 ds.$$

Using Assumption 2.2, the second term in (3.1) is dissipative:

$$\int_{t_0}^{t} f_2 (y')^2 ds \geq c_2 \int_{t_0}^{t} |y'(s)|^2 ds.$$

For the remaining integral terms, we use the growth conditions (Assumption 2.4) and Young's inequality ($ab \leq \varepsilon a^2 + \frac{1}{4\varepsilon} b^2$) for an arbitrary $\varepsilon > 0$:

$$\left| \int_{t_0}^{t} f_3 y y' ds \right| \leq \int_{t_0}^{t} C_3 (1 + |y|) |y'| ds \leq \varepsilon \int_{t_0}^{t} |y'|^2 ds + C_\varepsilon \int_{t_0}^{t} (1 + |y|^2) ds.$$

The term $\int (f_5 - f_4) y' ds$ is bounded similarly.
Substituting these estimates back into (3.1) and rearranging, we obtain:

$$\begin{aligned} \frac{c_1}{2} |y'(t)|^2 + c_2 \int_{t_0}^{t} |y'|^2 ds \leq & \frac{C_1}{2} |y_1|^2 + \frac{C_{1d}}{2} \int_{t_0}^{t} |y'|^2 ds \\ & + \varepsilon \int_{t_0}^{t} |y'|^2 ds + C_\varepsilon \int_{t_0}^{t} (1 + |y|^2) ds. \end{aligned}$$

Choosing ε small enough and applying Gronwall's inequality on the function $\int_{t_0}^{t} |y'(s)|^2 ds$, we find that $\int_{t_0}^{T} |y'(s)|^2 ds$ is bounded by a constant that depends on $\int_{t_0}^{T} |y(s)|^2 ds$ and the initial conditions. This in turn implies:

$$\sup_{t\in[t_0,T]} |y'(t)|^2 \leq C_1^* \left(1 + \int_{t_0}^{T} |y(s)|^2 ds \right). \tag{3.2}$$

Now we deal with the estimate of the solution $y(t)$.

Estimating the solution $y(t)$.
Next, we multiply Equation (2.1) by $y(t)$ and integrate:

$$\int_{t_0}^{t} f_1 y'' y ds + \int_{t_0}^{t} f_2 y' y ds + \int_{t_0}^{t} f_3 y^2 ds + \int_{t_0}^{t} f_4 y ds = \int_{t_0}^{t} f_5 y ds.$$

The key term is the one involving f_3. By Assumption 2.3:

$$\int_{t_0}^{t} f_3 y^2 ds \geq c_3 \int_{t_0}^{t} |y(s)|^2 ds.$$

The other terms can be bounded using integration by parts, the previous bound on $\sup |y'|$, and Young's inequality. For instance,

$$\int_{t_0}^{t} f_1 y'' y ds = [f_1 y' y]_{t_0}^{t} - \int_{t_0}^{t} (f_1' y y' + f_1 (y')^2) ds.$$

The boundary term $|f_1(t)y'(t)y(t)|$ can be bounded by $\varepsilon |y(t)|^2 + C_\varepsilon |y'(t)|^2$. After applying similar bounds to all other terms and absorbing the integral of $|y|^2$ to the left-hand side, we arrive at an inequality of the form:

$$\tilde{c} \int_{t_0}^{t} |y|^2 ds \leq C_2^* + \varepsilon \sup_{t \in [t_0, T]} |y(s)|^2.$$

Finally, using the Fundamental Theorem of Calculus, $y(t) = y_0 + \int_{t_0}^{t} y'(s) ds$, and the Cauchy-Schwarz inequality, we have:

$$|y(t)|^2 \leq 2|y_0|^2 + 2(T - t_0) \int_{t_0}^{t} |y'(s)|^2 ds.$$

Since we established that $\int |y'|^2$ is bounded (dependent on $\int |y|^2$), we can combine all inequalities. This forms a closed system of estimates, which implies that both $\sup |y(t)|^2$ and $\sup |y'(t)|^2$ must be bounded by a constant C that depends only on initial data and problem parameters.

Thus far, we proved that

$$\sup_{t \in [t_0, T]} |y(t)|^2 \leq C,$$
$$\sup_{t \in [t_0, T]} |y'(t)|^2 \leq C.$$

This achieve the required arguments for this proof.

□

4. Derivation of the Direct Block Hybrid Method

In this section, we derive the BHM for the direct numerical solution of the general second-order IVP:

$$y''(t) = G(t, y(t), y'(t)), \quad t \in [t_0, T] \tag{4.1}$$

with initial conditions $y(t_0) = y_0$ and $y'(t_0) = y_1$.

4.1. Method Formulation

We partition the interval $[t_0, T]$ into subintervals $[t_n, t_{n+1}]$ of step size h. Within each subinterval, we define a set of $m + 1$ collocation points $t_{n+\rho_i} = t_n + \rho_i h$, where $0 = \rho_0 < \rho_1 < \cdots < \rho_m = 1$. The core idea is to approximate the true solution $y(t)$ by a polynomial that collocates with the differential equation at these points.

The second derivative $y''(t)$ is approximated by a Lagrange interpolation polynomial passing through the collocation points:

$$y''(t_n + sh) \approx \sum_{j=0}^{m} y''(t_n + \rho_j h) L_j(s) = \sum_{j=0}^{m} G_{n+\rho_j} L_j(s), \tag{4.2}$$

where $G_{n+\rho_j} = G(t_{n+\rho_j}, y_{n+\rho_j}, y'_{n+\rho_j})$ and $L_j(s)$ is the Lagrange basis polynomial:

$$L_j(s) = \prod_{\substack{k=0 \\ k\neq j}}^{m} \frac{s - \rho_k}{\rho_j - \rho_k}.$$

Integrating Equation (4.2) once with respect to s from 0 to ρ_i yields an approximation for the first derivative $y'_{n+\rho_i}$:

$$y'_{n+\rho_i} = y'_n + h \sum_{j=0}^{m} \beta_{ij} G_{n+\rho_j}, \quad i = 1, 2, \ldots, m, \tag{4.3}$$

where the coefficients are given by $\beta_{ij} = \int_0^{\rho_i} L_j(s)ds$.
Integrating Equation (4.2) twice yields the formula for the solution $y_{n+\rho_i}$:

$$y_{n+\rho_i} = y_n + \rho_i h y'_n + h^2 \sum_{j=0}^{m} \alpha_{ij} G_{n+\rho_j}, \quad i = 1, 2, \ldots, m, \tag{4.4}$$

where the coefficients are $\alpha_{ij} = \int_0^{\rho_i} (\rho_i - s) L_j(s)ds$.
The coupled system of equations defined by (4.3) and (4.4) forms the BHM. This system simultaneously solves for the unknown values $\{y_{n+\rho_i}, y'_{n+\rho_i}\}_{i=1}^{m}$ within the block $[t_n, t_{n+1}]$.

4.2. Handling Nonlinearity with the Quasi-Linearization Method

Since the function $G(t, y, y')$ is generally nonlinear, the resulting system of algebraic equations is also nonlinear. To solve it efficiently, we employ the Quasi-Linearization Method (QLM). We linearize G around the previous iteration's values, denoted by (y_r, y'_r):

$$G(t, y, y') \approx G_r + (y - y_r)\phi_r + (y' - y'_r)\chi_r, \tag{4.5}$$

where $G_r = G(t, y_r, y'_r)$, $\phi_r = \frac{\partial G}{\partial y}|_{(y_r, y'_r)}$, and $\chi_r = \frac{\partial G}{\partial y'}|_{(y_r, y'_r)}$. This can be rewritten as:

$$G(t, y, y') \approx \psi_r + y\phi_r + y'\chi_r, \tag{4.6}$$

where $\psi_r = G_r - y_r\phi_r - y'_r\chi_r$ and

$$\psi_r = G_r - \frac{\partial G_r}{\partial X_r} X_r - \frac{\partial G_r}{\partial X'_r} X'_r,$$
$$\phi_r = \frac{\partial G_r}{\partial X_r},$$
$$\chi_r = \frac{\partial G_r}{\partial X'_r}.$$

Substituting this linearized form into the BHM equations (4.3) and (4.4) results in a linear system of $2m \times 2m$ equations for the unknowns $(y_{n+\rho_i}, y'_{n+\rho_i})$ at each iteration of the QLM. In matrix-vector form, this system can be expressed as:

$$\begin{bmatrix} A_{11} & A_{12} \\ A_{21} & A_{22} \end{bmatrix} \begin{bmatrix} \mathbf{Y}_n \\ \mathbf{Y}'_n \end{bmatrix} = \begin{bmatrix} \mathbf{R}_1 \\ \mathbf{R}_2 \end{bmatrix}, \tag{4.7}$$

where $\mathbf{Y}_n = [y_{n+\rho_1}, \ldots, y_{n+\rho_m}]^T$, $\mathbf{Y}'_n = [y'_{n+\rho_1}, \ldots, y'_{n+\rho_m}]^T$, and the matrices A_{ij} and vectors $\mathbf{R}_k$ depend on the coefficients α_{ij}, β_{ij}, the step size h, and the known values from the previous time step t_n. This linear system can be solved efficiently at each QLM iteration until convergence is achieved.

5. Numerical Experiments

In this section, we validate the performance of the direct BHM on several benchmark second-order nonlinear IVPs. The method was implemented using four collocation points ($\rho_i \in \{0, 1/4, 3/4, 1\}$). For problems without a known exact solution, the numerical solution obtained from MATLAB's highly accurate 'ode45' solver with very stringent tolerances is used as a reference.

Example 5.1 (Forced Duffing Equation) *We first consider the Duffing equation with a known analytical solution, previously studied in [18]:*

$$y''(x) = -y'(x) - y(x) - y(x)^2 y'(x) + 2\cos(x) - \cos^3(x), \quad x \in [0, 10]$$

with initial conditions $y(0) = 0, y'(0) = 1$. The exact solution is $y(x) = \sin(x)$.

The above problem was investigated first in the paper [11] and most recently in the work [18]. We obtained the same result as in [18, p. 537]. Note that this is a particular case of the problem we are dealing with in this paper. For the block hybrid approach to work, we derive the functions below:

$$\begin{aligned} \psi_r &= 2y_r^{'} - 2y_r + 2y_r^2 y_r^{'} + 2\cos(x) - \cos^3(x) \\ \phi_r &= -(1 + 2y_r y_r^{'}) \\ \chi_r &= -(1 + y_r^2). \end{aligned}$$

Figure 1 shows a perfect agreement between the BHM numerical solution and the exact solution for both $y(x)$ and $y'(x)$. The error plot in Figure 2 confirms the high accuracy of the method, with the maximum absolute error remaining on the order of 10^{-8}. The phase portrait further illustrates that the numerical solution accurately captures the periodic dynamics of the system.

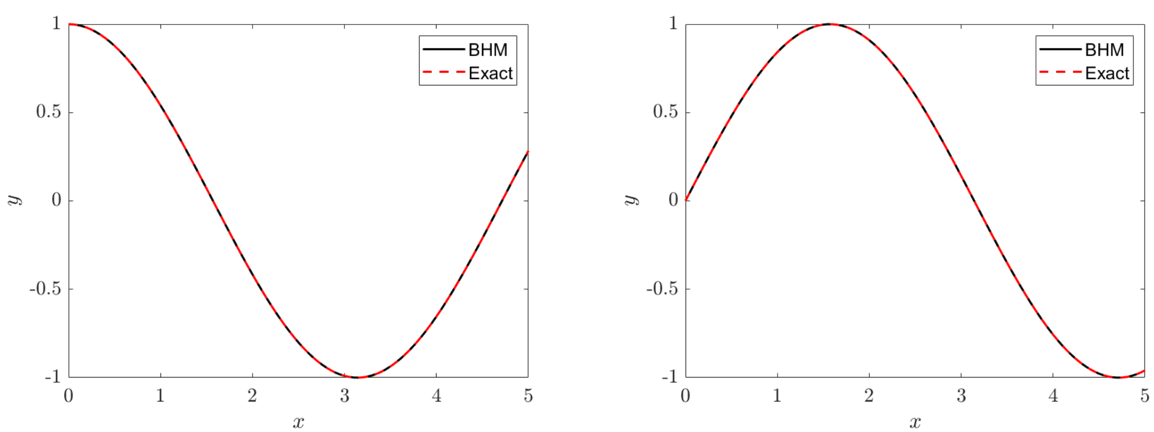

a Solution $y(x)$ vs. exact solution. b Derivative $y'(x)$ vs. exact solution.

Figure 1: Numerical and exact solutions for the Duffing equation (Example 5.1).

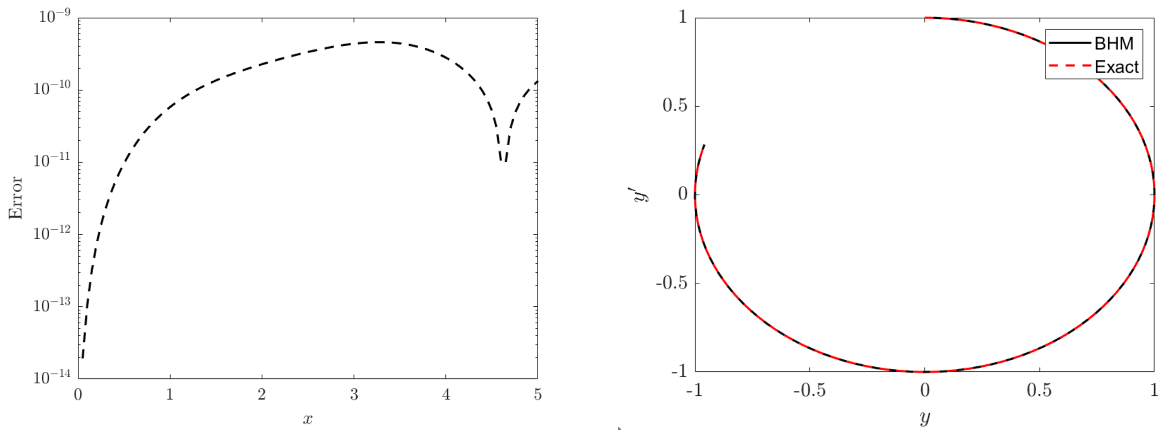

a Absolute error of the numerical solution.

b Phase portrait (y' vs. y).

Figure 2: Error analysis and phase portrait for the Duffing equation (Example 5.1).

Example 5.2 (Custom Nonlinear Oscillator) *Next, we consider a highly nonlinear oscillator equation without a known analytical solution:*

$$y''(t) = -\left(\frac{4}{3} + 3y(t)^2\right) - \frac{1}{3}y(t) - y(t)^3 \text{ with } y(0) = 0, y'(0) = 0.5.$$

The approximate functions are:

$$\begin{aligned} \psi_r &= -\frac{4}{3} + 3y_r^2 + 2y_r^3, \\ \phi_r &= -(6y_r + \frac{1}{3} + 3y_r^2), \\ \chi_r &= 0. \end{aligned}$$

The results are shown in Figure 3. The BHM solution closely follows the reference solution from "ode45". The phase portrait reveals complex, non-periodic oscillatory behavior, which our method successfully captures. This example demonstrates the robustness of the BHM in handling equations with strong polynomial nonlinearities.

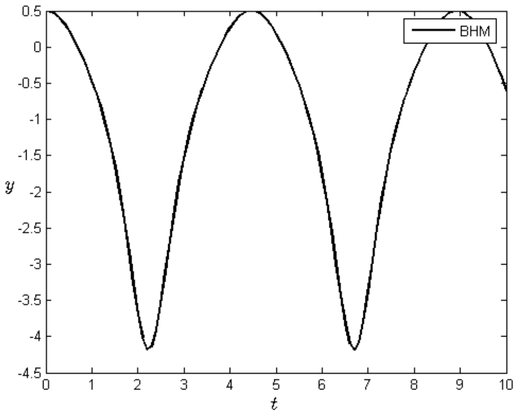

a Numerical solution $y(t)$ vs. reference.

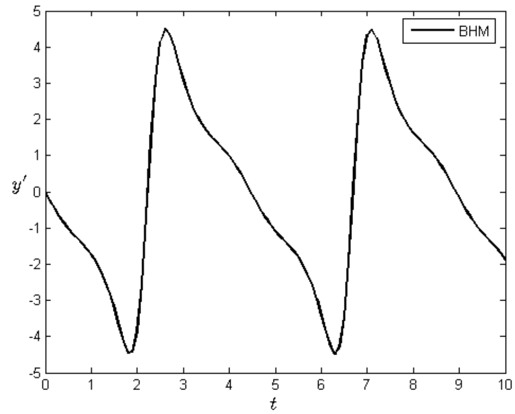

b Numerical derivative $y'(t)$ vs. reference.

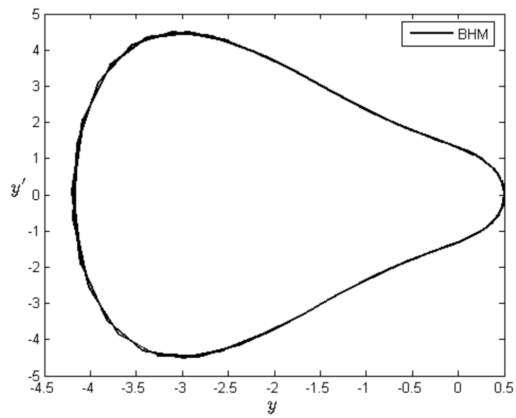

c Phase portrait (y' vs. y).

Figure 3: Numerical results for the custom nonlinear oscillator (Example 5.2).

Example 5.3 (Generalized Van der Pol Equation with Damping) *We now solve another generalized Van der Pol equation that includes nonlinear damping:*

$$y''(t) = -\left(\frac{4}{3} + 3y(t)^2\right) y'(t) - \frac{1}{3}y(t) - y(t)^3, \text{ with } y(0) = 0, y'(0) = 0.5.$$

The approximate functions are:

$$\psi_r = -\frac{1}{3} + 6y_r^2 + 2y_r^3,$$
$$\phi_r = -(6y_r + \frac{1}{3} + 3y_r^2),$$
$$\chi_r = -\left(\frac{4}{3} + 3y_r^2\right).$$

Figure 4 illustrates the method's ability to handle nonlinear damping terms accurately. The solution exhibits damped oscillations, and the phase portrait shows the trajectory spiraling towards a stable fixed point at the origin. The BHM solution is visually indistinguishable from the reference solution, confirming its reliability for this class of problems.

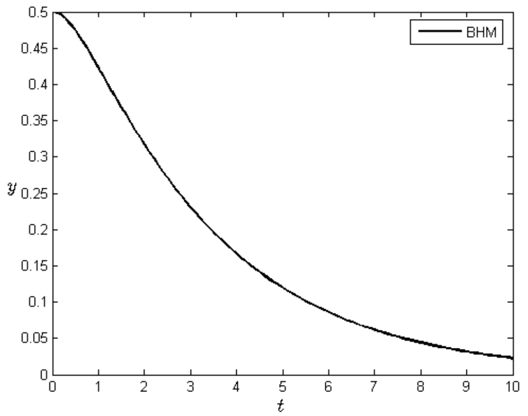

a Numerical solution $y(t)$ vs. reference.

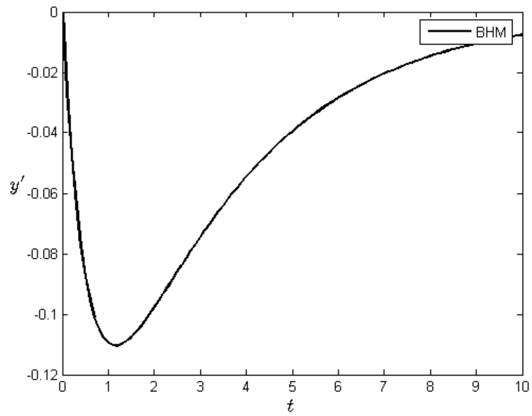

b Numerical derivative $y'(t)$ vs. reference.

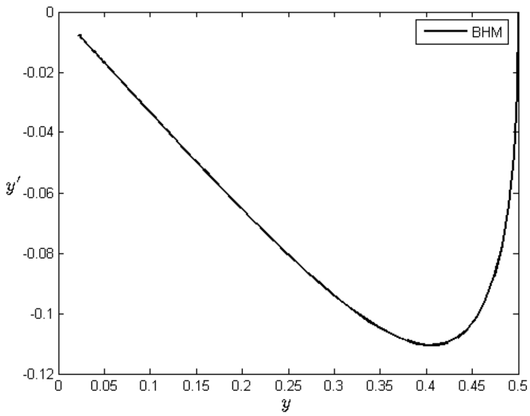

c Phase portrait (y' vs. y).

Figure 4: Numerical results for the generalized Van der Pol equation (Example 5.3).

In this case we compare our results with the work in [13, Example 7.2 on page 11] of analytical and numerical solutions in the paper from [13].

We must emphasize that the work in this manuscript generalizes to some extend most results that can be found in the papers [1], [6], [7], [17], [16], [18], [**?**] and [8]. In all cases, the proposed Block Hybrid numerical Method converges much faster and it is more efficient. The obtained error for the given solutions are sufficiently small enough to validate the accuracy.

Example 5.4 *In order to solve the below (Example 5.5) IVP, we first solve the homogeneous case of the generalized IVP:*

$$\frac{d^2y}{dt^2} + \alpha(y^2 - 1)\frac{dy}{dt} + y = 0, \text{ with } y(0) = 0 \text{ and } y'(0) = 2.$$

The exact solutions is given by: $y(t) = 2\sin(t)$ *and the approximate functions:*

$$\begin{aligned} \psi_r &= 2\alpha y_r^2 y_r^{'}, \\ \phi_r &= -2\alpha y_r y_r^{'} - 1, \\ \chi_r &= -\alpha(y_r^2 - 1). \end{aligned}$$

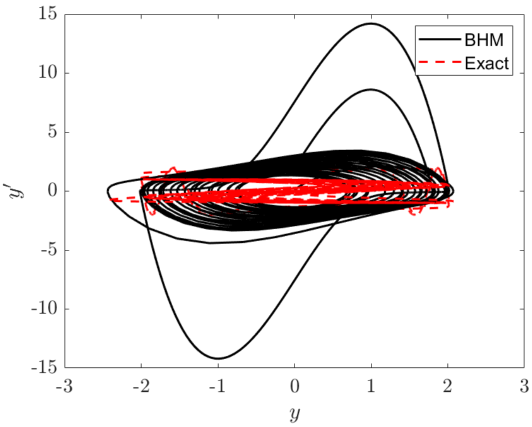

a $\varepsilon = 1.02$: Resonance curves, $\omega = 1$, $n = 0$.

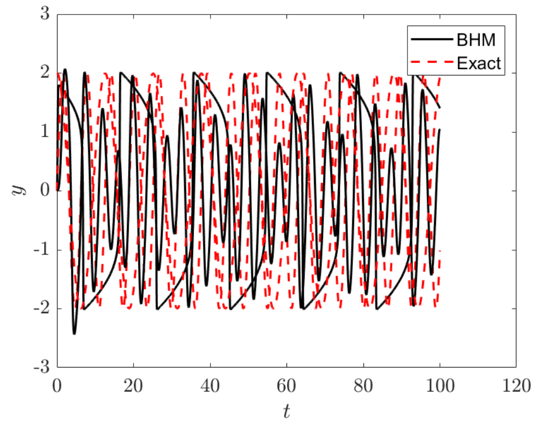

b $\varepsilon = 10$: Comparison of y' and its BHM derivative.

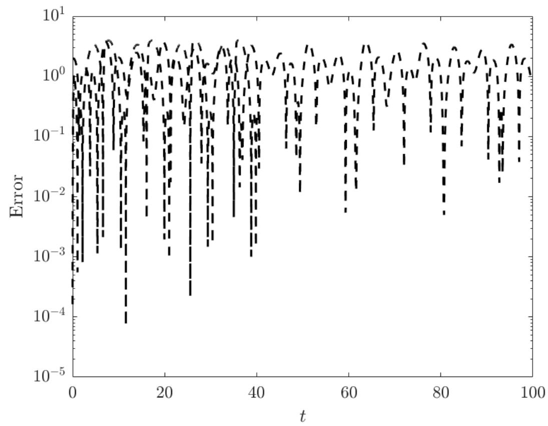

c $\varepsilon = 10$: Error estimation

Figure 5: Numerical results for the generalized Van der Pol equation (Example 5.4).

Example 5.5 *We consider the differential equation in this example*

$$\frac{d^2y}{dt^2} + \alpha(y^2 - 1)\frac{dy}{dt} + y = F(t)$$

where $F(t) = \Omega_0 \cos(\omega t)$ *the* $\varepsilon > 0$ *and* Ω_0 *is the amplitude. This problem is supplemented with the initial conditions* $y(0) = 2$ *and* $y'(0) = 0$*. And the exact solution is given by:* $y(t) = 2\cos(\omega t)$*.*

We can now derive the following functions for the Block Hybrid approximation:

$$\begin{aligned}
\psi_r &= G_r - y_r \frac{dG_r}{dy_r} - y_r^{'} \frac{dG_r}{dy_r^{'}} = 2\alpha y_r^2 y_r^{'} + \Omega_0 \cos(\omega t), \\
\phi_r &= \frac{dG_r}{dy_r} = -2\alpha y_r y_r^{'} - 1, \\
\chi_r &= \frac{dG_r}{dy_r^{'}} = \alpha(1 - y_r^2).
\end{aligned}$$

In this particular case we take different values for the parameter $\alpha := 0.1$

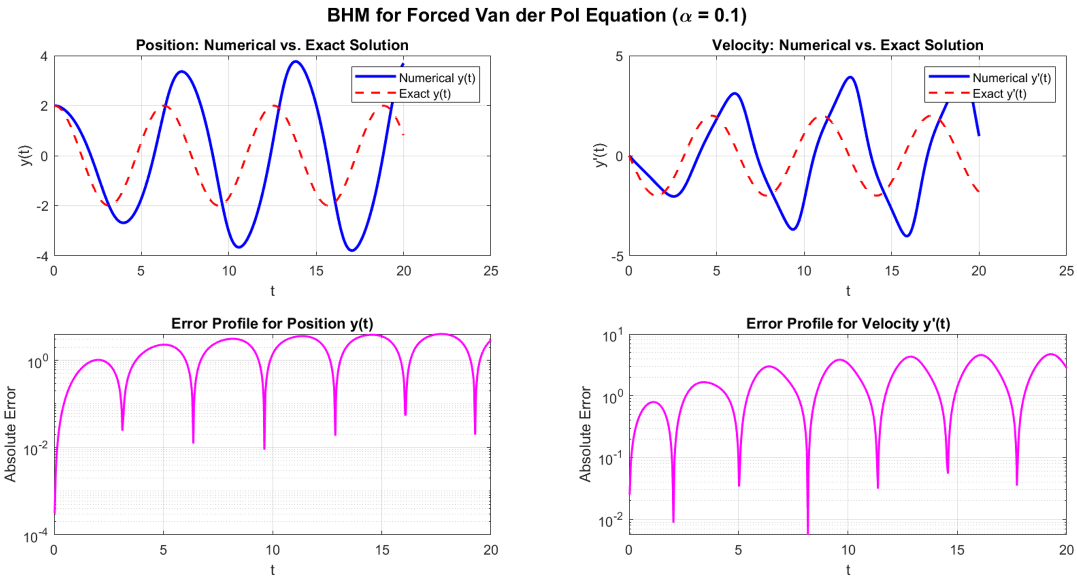

Figure 6: Numerical approximation with $\alpha := 0.1$

For $\alpha = 1$ we obtain the figure below which shows that our method even performs much better than the results in [8].

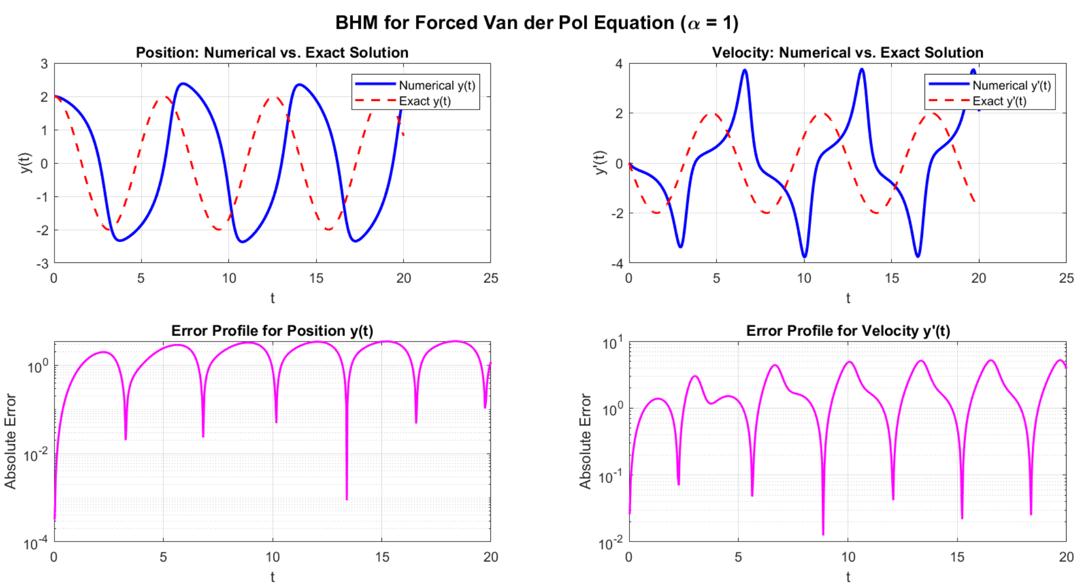

For the case $\alpha = 0.01$ we obtain the figure below which shows that our method even performs much better than the results in [8].

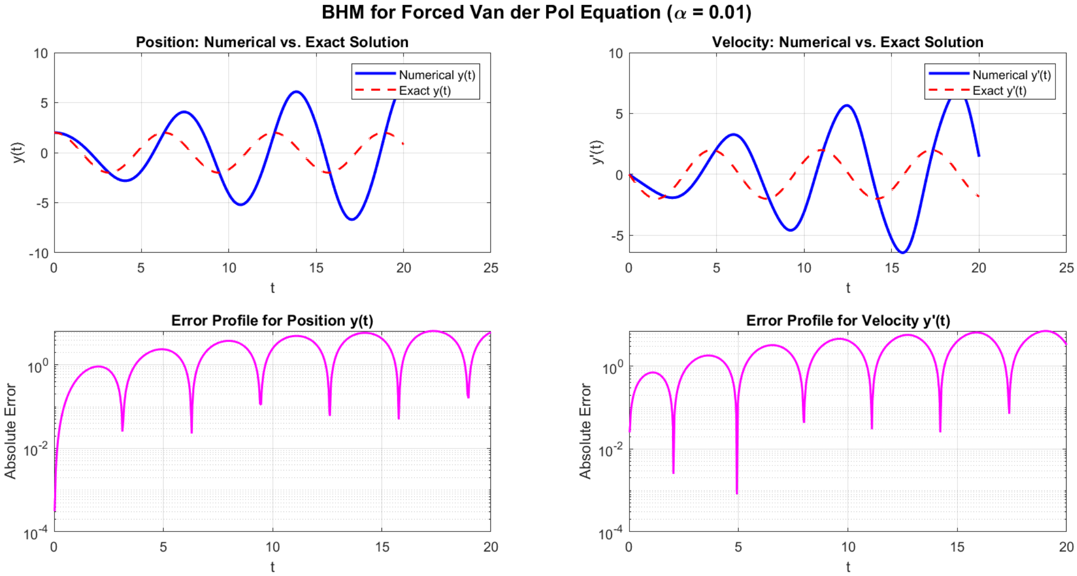

For $\alpha \equiv 1$ we notice that our result matches the same result of Figure (a) in the paper [19] as it can be seen in the figure below.

Note that for $\alpha = 10$, we reach the period much faster that the result obtained in Figure (b) in the paper [8] and [19], as well as the result in [6]. It is worth noticing that as in [6], we only needed a time $t = 50$ as compared to the result in [8] and [19] which required $t = 120$ a much more bigger than the double interval.

This literally confirm that the BHM converges faster to the exact solution than any other method.

Note for $\alpha \equiv 100$ and $\alpha \equiv 200$ we obtain the results in the figure below which match the results in Figures (c) and (d) of [3] and [6]. Our results converges faster since our interval is much smaller as compared to the interval used in [3], and [6].

As for the derivatives we also got the same results for different values of $\alpha = 1, 10, 100, 200$.

Note that for $\varepsilon = 100$ and $\varepsilon = 200$ we practically get the same result in the figure below. It is worth noting that the interval of convergence for the BHM is sufficiently small as compared to the other methods.

Example 5.6

$$\frac{d^2y}{dt^2} - \alpha(1 - y^2)\frac{dy}{dt} + \omega_1^2 y = \omega_1^2 E \sin(n\omega_1 t)$$

with $\varepsilon = \frac{\alpha}{\omega_1} \gg 1$ for $n = 3$, the exact solution $y(t) = 2\cos(\omega_1 t)$ and $E = 2\varepsilon$.

For the Hybrid scheme, we derive the following functions:

$$\begin{aligned}
\psi_r &= G_r - y_r \frac{dG_r}{dy_r} - y_r^{'} \frac{dG_r}{dy_r^{'}} = 2\alpha y_r^2 y_r^{'} + \omega_1^2 E \sin(n\omega_1 t) \\
\phi_r &= \frac{dG_r}{dy_r} = -2\alpha y_r y_r^{'} - \omega_1^2, \\
\chi_r &= \frac{dG_r}{dy_r^{'}} = \alpha(1 - y_r^2).
\end{aligned}$$

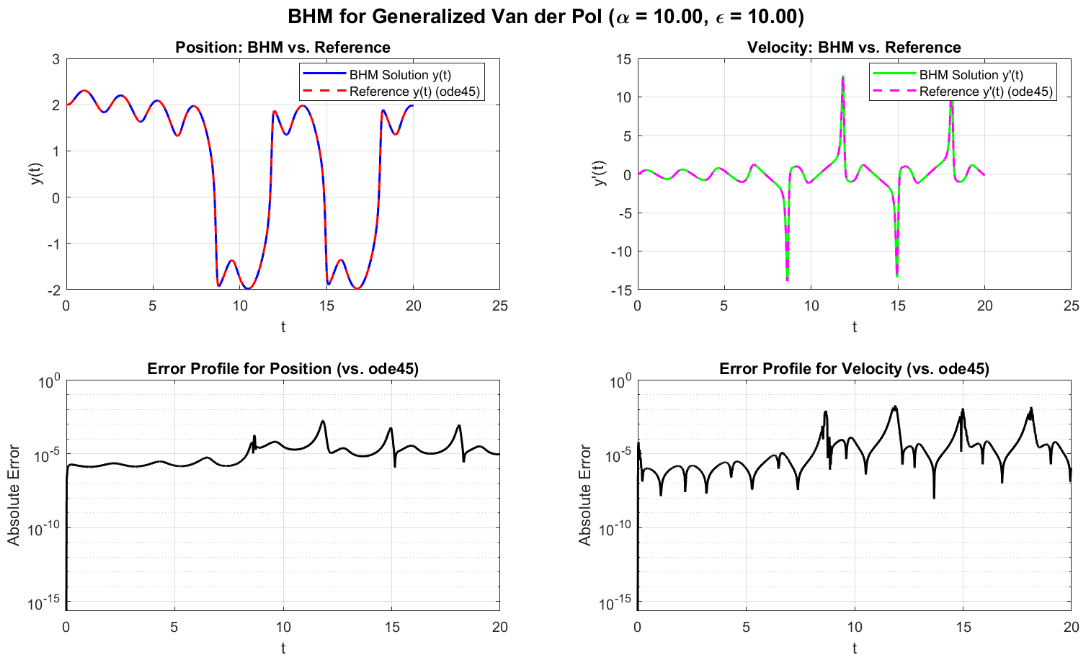
BHM for Generalized Van der Pol (α = 10.00, ϵ = 10.00)
Position: BHM vs. Reference
BHM Solution y(t)
Reference y(t) (ode45)
y(t)
t
Velocity: BHM vs. Reference
BHM Solution y'(t)
Reference y'(t) (ode45)
y'(t)
t
Error Profile for Position (vs. ode45)
Absolute Error
t
Error Profile for Velocity (vs. ode45)
Absolute Error
t

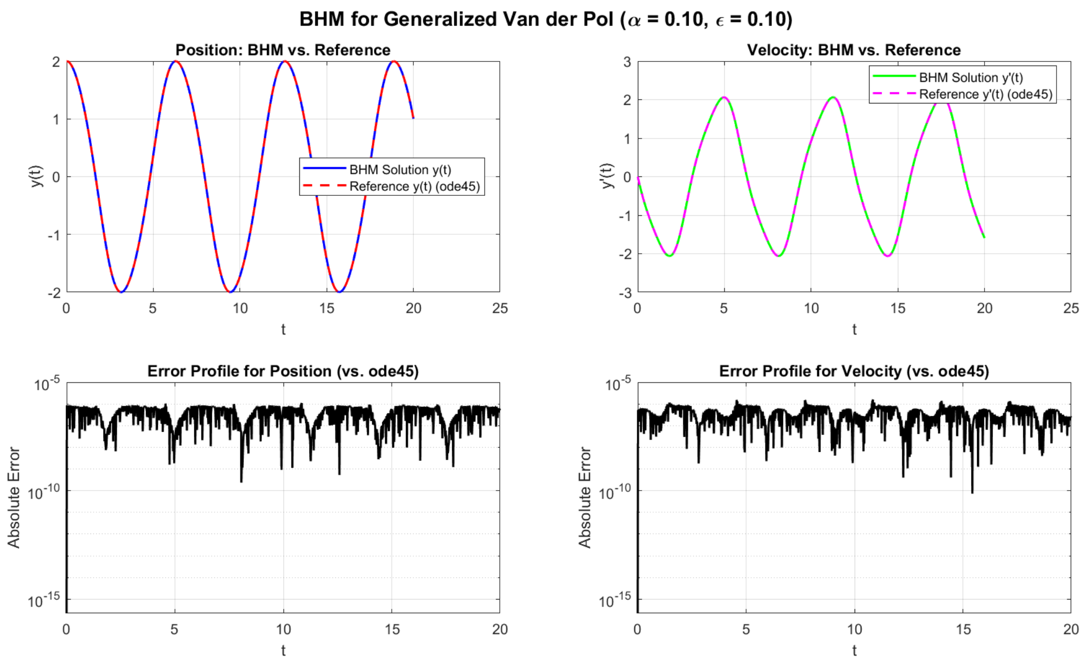
BHM for Generalized Van der Pol (α = 0.10, ϵ = 0.10)
Position: BHM vs. Reference
BHM Solution y(t)
Reference y(t) (ode45)
y(t)
t
Velocity: BHM vs. Reference
BHM Solution y'(t)
Reference y'(t) (ode45)
y'(t)
t
Error Profile for Position (vs. ode45)
Absolute Error
t
Error Profile for Velocity (vs. ode45)
Absolute Error
t

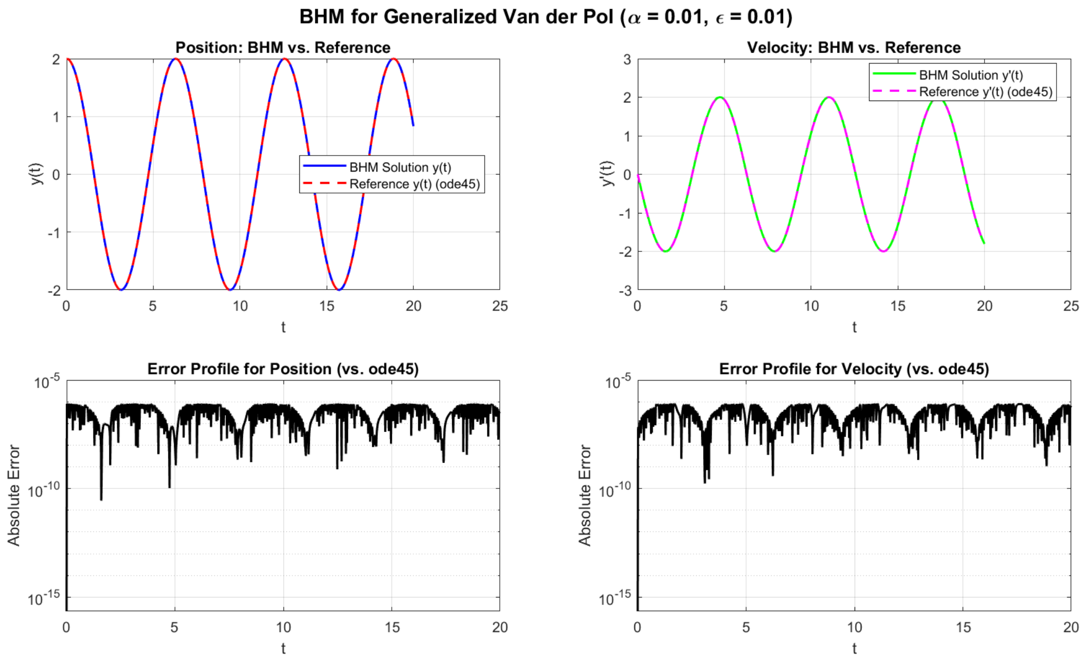

Example 5.7 *We further consider the nonlinear singular initial value problem of the form*

$$\frac{d^2y}{dt^2} = -\frac{\cos t}{\sin t}\frac{dy}{dt} + \alpha y - 2\beta\cos t \tag{5.1}$$

subjected to the initial conditions $y(0) = 1$ and $y'(0) = 0$.

We observe that this is a very interesting problem because it involves a singular initial value problem. Namely, the coefficient term $\cos(t)/\sin(t)$ (or $\cot(t)$) is undefined at the initial time $t = 0$, which makes this a challenging case for standard numerical solvers. In order for us to directly address this issue, we tackle the key points: handling the singularity at $t = 0$ as well as finding the exact solution for verification. To handle the singularity, we note that a direct evaluation of the RHS of (5.1) at $t = 0$ will result in a division by zero error. However, this is a removable singularity which can be easily addressed using l'Hospital rules. To find the exact solution, we forced the problem to admit an exact solution by carefully choosing the parameters α and β. Using the guessing techniques, if we set $y(t) = cos(t)$, then $y(0) = 1$, $y'(0) = 0$ (matching the initial conditions). Then we observe that $y' = -sin(t)$, and $y'' = -cos(t)$. Substituting this into the problem (5.1) gives:

$$\begin{aligned} -\cos(t) &= -(\cos(t)/\sin(t)) * (-\sin(t)) + \alpha\cos(t) - 2\beta\cos(t), \\ -\cos(t) &= \cos(t) + (\alpha - 2\beta)\cos(t) \end{aligned}$$

This holds if -1 = 1 + α - 2 β, which simplifies to the condition: $\alpha - 2\beta = -2$.

In order for us to create a valid test case, we choose parameters that satisfy this condition, for example, $\alpha = 2$ and $\alpha = 2$. This makes $y(t) = cos(t)$ the true exact solution, allowing for a precise error analysis of our BHM solver.

We need to emphasis that, as we astutely noted, this exact solution only works for the aforementioned special case imposed on the parameters α and β. For the general problem, we need to rely on the numerical comparative approach to approximate the solution. This tells us that more importantly, for a general choice of α and β, there is no simple analytical solution.

The approximating functions are given by

$$
\begin{aligned}
\psi_r &= G_r - y_r \frac{dG_r}{dy_r} - y_r^{\prime} \frac{dG_r}{dy'} = -2\beta\cos(t),\\
\phi_r &= \frac{dG_r}{dy_r} = \alpha,\\
\chi_r &= \frac{dG_r}{dy_r'} = -\frac{\cos t}{\sin t}.
\end{aligned}
$$

The figure below provides a clean and direct assessment of our BH method's accuracy for this singular IVP. We observe that the exact solution and the BHM approximation matches each other initially until certain time $t = 18$ before drifting apart.

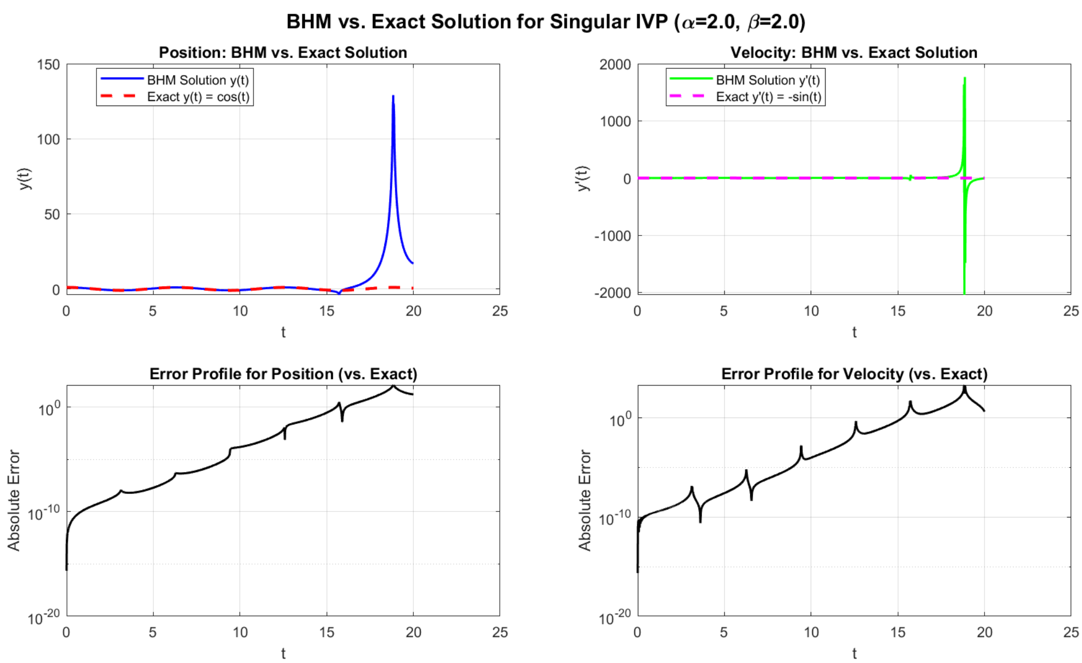

Due to the above observation, for any other choice of the parameters α and β, our singular IVP does not have a solution. This is why for the general case, we must compare against a numerical reference like "ode45". It is noteworthy to mention that our singular IVP cannot be solved using the well-known, ADM nor its modified version nor the Runger Kuta scheme. In order to implement the ADM, it becomes non-trivial for this singular challenging IVP, to use it, it would requires symbolic integration techniques. In the figure below, we obtained the plots showing the BHM solution compared with the reference solution obtained from "ode45" as well as the absolute error between them.

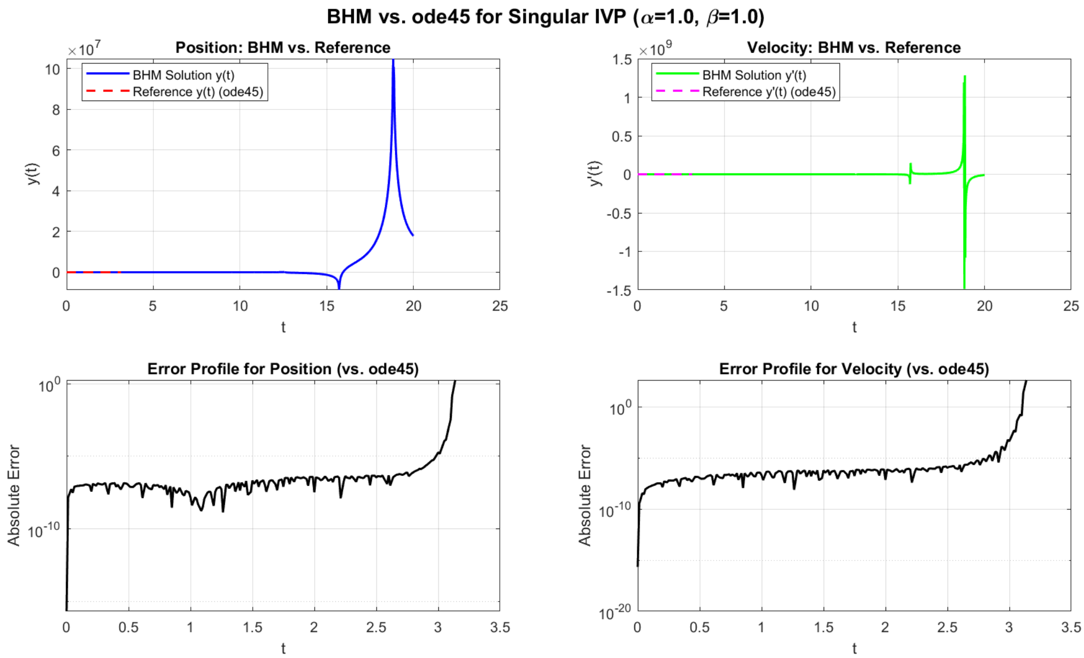

Example 5.8

$$\frac{d^2y}{dt} - \alpha(1-y^2) = \omega_1^2 E \sin(n\omega_1 t)$$

with $\varepsilon = \frac{\alpha}{\omega_1} \gg 1$ *for* $n = 3$*, the exact solution* $y(t) = 2\cos(\omega_1 t)$ *and* $E = 2\varepsilon$*. The approximating functions are given by:*

$$\psi_r = G_r - y_r \frac{dG_r}{dy_r} - y_r^{'} \frac{dG_r}{dy_r^{'}} = \alpha(1+y_r^2) + \omega_1^2 E \sin(n\omega_1 t)$$
$$\phi_r = \frac{dG_r}{dy_r} = -2\alpha y_r,$$
$$\chi_r = \frac{dG_r}{dy_r^{'}} = 0.$$

We take $\alpha \ggg 1$*, we observe that*

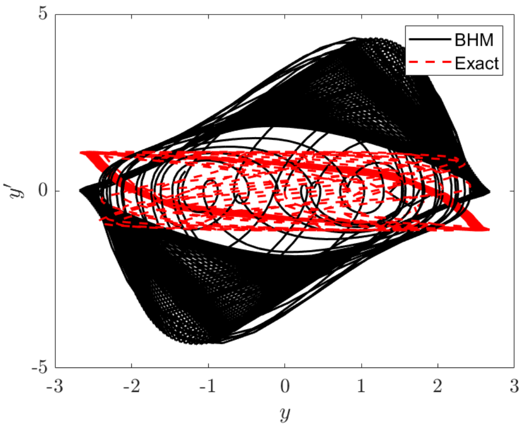

a $\alpha = 1.02$: Resonance curves, $E = 2\alpha$, $\omega = 0.5546$, $n = 3$

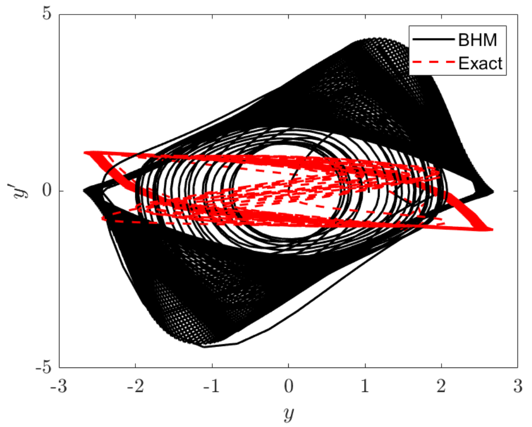

b $\alpha = 1.02$: Error estimation, $E = 2\alpha$, $\omega = 0.5546$, $n = 1$

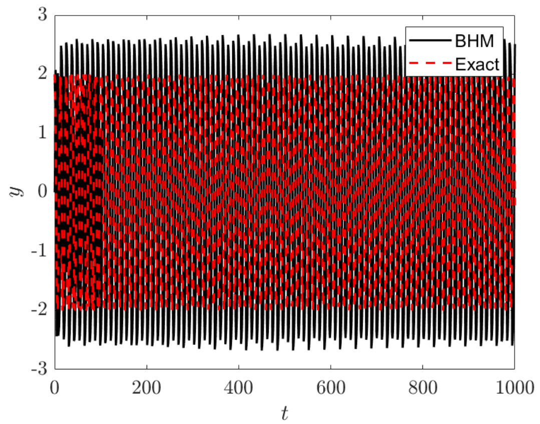

c $\alpha = 1.02$: Solution $y(t)$ vs BHM, $E = 2\alpha$, $\omega = 0.5546$, $n = 3$

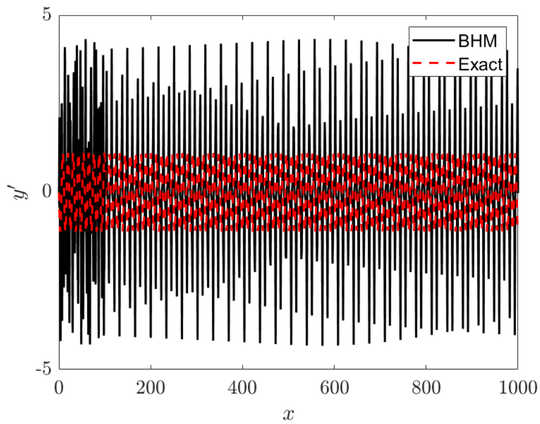

d $\alpha = 1.02$: Derivative y' vs t, $E = 2\alpha$, $\omega = 0.5546$, $n = 3$

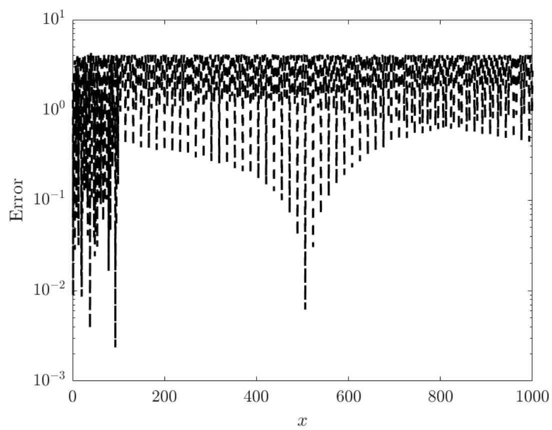

e $\alpha = 1.02$: Error estimation, $E = 2\alpha$, $\omega = 0.5546$, $n = 3$

Figure 7: Numerical results for the generalized Van der Pol equation (Example 5.12), showing system dynamics and error analysis under different conditions.

6. Conclusion

In this paper, we have successfully developed and implemented a direct Block Hybrid Method for solving a general class of second-order nonlinear initial value problems, including the canonical Van der Pol and Duffing oscillator equations.

The key strengths of our approach are its ability to solve second-order ODEs directly without increasing the system's dimensionality and its block-based formulation that enhances computational efficiency. The theoretical analysis provided a priori estimates, ensuring the boundedness of the solutions under general conditions and giving a solid mathematical foundation to the numerical scheme.

The numerical experiments demonstrated the method's high accuracy and robustness. For problems with known analytical solutions, the BHM produced results with very small errors. For highly nonlinear problems without exact solutions, our method's results were in excellent agreement with those from a high-precision reference solver. The method proved capable of accurately capturing diverse dynamical behaviors, from simple periodic oscillations to complex damped and nonlinear dynamics.

Based on these findings, we conclude that the direct Block Hybrid Method, combined with the Quasi-Linearization Method, is an efficient, accurate, and reliable tool for the numerical integration of second-order nonlinear differential equations. It stands as a powerful alternative to traditional methods and is well-suited for a wide range of applications in science and engineering.

Acknowledgments

We are grateful to the anonymous reviewers for their insightful comments and constructive suggestions, which have greatly improved the quality and presentation of this article.

References

1. Z. Abdul Majid, N.Z. Mokhtar, and M. Suleiman, *Direct Two-Point Block One-Step Method for Solving General Second-Order Ordinary Differential Equations*, Math. Probl. Eng. **2012** (2012), 184253.
2. O. Adeyeye and Z. Omar, *Solving third order ordinary differential equations using one-step block method with four equidistant generalized hybrid points*, IAENG Internat. J. Appl. Math. **49** (2019), no. 2, 1–9.
3. S.A. Ahmedai Abd Allah, P. Sibanda, S.P. Goqo, U.O. Rufai, H. Sithole Mthethwa, and O.A. Noreldin, *A Block Hybrid Method with Equally Spaced Grid Points for Third-Order Initial Value Problems*, AppliedMath **4** (2024), no. 1, 320–347.
4. G. Ajileye, S.A. Amoo, and O.D. Ogwumu, *Hybrid block method algorithms for solution of first order initial value problems in ordinary differential equations*, J. Appl. Comput. Math. **7** (2018), no. 2, 1–4.
5. M. Alkasassbeh and Z. Omar, *Implicit One-Step Block Hybrid Third-Derivative Method for the Direct Solution of Initial Value Problems of Second-Order Ordinary Differential Equations*, J. Appl. Math. **2017** (2017), 8510948.
6. Z. Ali, T. Sekgobela, and F. Nyathi, *Numerical Approximation of the Generalized Van Der Pol Equations.* Available at SSRN 4995890.
7. R. Allogmany and F. Ismail, *Direct solution of* $u'' = f(t, u, u')$ *using three point block method of order eight with applications*, J. King Saud Univ.-Science **33** (2021), no. 2, 101337.
8. A.O. Elnady, A. Newir, and M.A. Ibrahim, *Novel approach for solving higher-order differential equations with applications to the Van der Pol and Van der Pol–Duffing equations*, Beni-Suef Univ. J. Basic Appl. Sci. **13** (2024), no. 1, 29.
9. J.M. Ginoux, *Van der Pol's Method: A Simple and Classic Solution*, History of Nonlinear Oscillations Theory in France (1880-1940), Springer, Cham, 2017, pp. 275–289.
10. J. Guckenheimer, K. Hoffman, and W. Weckesser, *The forced van der Pol equation I: The slow flow and its bifurcations*, SIAM J. Appl. Dyn. Syst. **2** (2003), no. 1, 1–35.
11. M. Khalid, M. Sultana, U. Arshad, and M. Shoaib, *A comparison between new iterative solutions of non-linear oscillator equation*, Internat. J. Comput. Appl. **128** (2015), no. 4, 1–5.
12. M.I. Modebei, S.N. Jator, and H. Ramos, *Block hybrid method for the numerical solution of fourth order boundary value problems*, J. Comput. Appl. Math. **377** (2020), 112876.
13. M. Mohammadi, A.R. Vahidi, T. Damercheli, and S. Khezerloo, *Numerical solutions of Duffing van der Pol equations on the basis of hybrid functions*, Adv. Math. Phys. **2023** (2023), 4144552.
14. M.O. Ogunniran, G.C. Olaleye, O.A. Taiwo, A. Shokri, and K. Nonlaopon, *Generalization of a class of uniformly optimized k-step hybrid block method for solving two-point boundary value problems*, Results Phys. **44** (2023), 106147.
15. H. Ramos, *An optimized two-step hybrid block method for solving first-order initial-value problems in ODEs*, Differential Geom. Dyn. Syst. **19** (2017), 107–118.

16. A.F.N. Rasedee, M.H. Abdul Sathar, K.I. Othman, S.R. Hamzah, and N. Ishak, *Approximating non linear higher order ODEs by a three point block algorithm*, Plos One **16** (2021), no. 2, e0246904.

17. A.F.N. Rasedee, M.H. Abdul Sathar, T.J. Wong, L.F. Koo, and N.A. Ramli, *Numerical solution for Duffing-Van Der Pol oscillator via block method*, Adv. Math. Sci. J. **10** (2021), no. 1, 19–28.

18. A.F.N. Rasedee, M.H. Abdul Sathar, N. Najib, N.M. Jan, S.M. Mohd, and S.N.A.M. Aslam, *Three-Point Block Algorithm for Approximating Duffing Type Differential Equations*, Stat. Optim. Inf. Comput. **10** (2022), no. 3, 529–541.

19. A.S. Soomro, G.A. Tularam, and M.M. Shaikh, *A comparison of numerical methods for solving the unforced van der Pol's equation*, Math. Theory Model. **3** (2013), no. 2, 66–77.

Zakaria Idriss Ali, Freeman Nyathi and Thaithai Sekgobela,

Department of Mathematical Sciences,

College of Science, Engineering and Technology, University of South Africa

South Africa.

E-mail address: alizi@unisa.ac.za

E-mail address: nyathif@unisa.ac.za

E-mail address: Esekgotw@unisa.ac.za